THE JOURNAL OF PHYSICAL CHEMISTRY C

Article

pubs.acs.org/JPCC

# Single-Molecule Conductance through Chiral Gold Nanotubes

Arijit Sen,[†,§] Chun-Ju Lin,[†] and Chao-Cheng Kaun*[,†,‡]

[†]Research Center for Applied Sciences, Academia Sinica, Taipei 11529, Taiwan

[‡]Department of Physics, National Tsing-Hua University, Hsinchu 30013, Taiwan

**ABSTRACT:** Using first-principles calculations based on the density functional theory and the nonequilibrium Green's functions approach, we demonstrate that single-molecule junctions can be constructed by chiral single-wall gold nanotubes, which display different transmission spectra from the ones based on achiral gold nanowires. The character of the molecule (viz. $\sigma$- or $\pi$-type) features the main conduction channel, determining the distribution of local density of states, which can be controlled further by the chirality of the electrodes. Calculated conductance values being in good accord with the available measured data indicates that our analysis can shed light into the viable junction geometries and their conduction mechanisms.

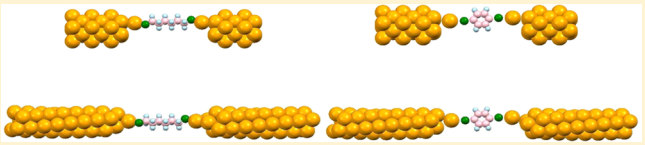

## INTRODUCTION

A key issue involving the progress of molecular electronics[1−3] lies in how effectively we can harness the desired structure−function relationship at the nanoscale, so as to reduce the gap between theory and experiment. To this end, a detailed understanding of the conduction properties of a single-molecule junction, consisting of a molecule bridging two electrodes, is required. While contributions of diverse molecules and molecule−electrode contacts on junction conductance have remained the focus of active theoretical research in recent years,[4−11] only a few studies address the roles played by the electrodes.[12−15] As the gold tip of a scanning probe microscope is retracted from the molecule, the gold nanowires along with the atomic contact develop at the ends of the molecule[16] so that the single-molecule conductance can be measured.[17−22] The electromigration technique also provides a route to generate nanowires[23] and measure conductance.[24] These nanowires, together with the molecule and contacts, form the conduction bottleneck of the whole system (including the mesoscopic electrodes which connect to the outside world), and their fine structures can affect the conductance of the junction. For example, the orientations of these gold nanowires have a strong likelihood along the [100] and [111] directions[25] and could cause the high and low conductance, respectively, in an alkanedithiolate single-molecule junction.[15]

Chiral single-wall gold nanotubes may well constitute the narrowed electrodes in a single-molecule junction, since such a tube, suspended between two gold leads, exists due to its local minimum in the string tension.[26,27] Atomic structures of $(n,m)$ gold nanotubes can be obtained by cylindrical folding of the 2D triangular lattice, where $n$ and $m$ denote the number of helical strands and the chirality, respectively.[27] The (5,3) gold nanotube, a long-lived metastable structure, has been observed experimentally,[28] which possesses five ballistic conduction channels near the Fermi level, with different periods and directions of chirality, resulting in mixed conduction properties.[27] However, when a single molecule bridges these nanotubes, the molecular moiety behaves as a momentum filter, and a particular conduction channel can be chosen, such as the $\sigma$ and $\pi$ channel in alkanedithiolate and benzenedithiolate (BDT) molecular junctions, respectively.[12,13] These characters offer novel transport properties in a single-molecule junction. For instance, the periodicity of a channel may influence the wavelength of the incident electron wave, and thus the coupling strength of the junction. To the best of our knowledge, the conductance and transport properties of a chiral-electrode junction have not been addressed yet.

While the computed and the measured conductance values agree quantitatively well in molecular junctions formed by a $\sigma$-saturated alkanedithiolate molecule,[15,29,30] similar agreement in a junction built by a $\pi$-conjugated molecule has only been achieved in a few weakly coupled systems, such as oligophenyldiamine[10] and bipyridine,[11] with the help of the GW approximation. In a strongly coupled junction, such as BDT, where aligning the broadened molecular level with the electrode Fermi level self-consistently is essential, discrepancy between theory and experiment, however, still occurs.[31−33] When the isolated molecule couples with leads, the metal-induced gap states[15] emerge between the highest occupied molecular orbital (HOMO) and the lowest unoccupied molecular orbital (LUMO), and dominate the junction conductance, which can be calculated self-consistently and accurately. Here we consider atomistic details in hexanedithiolate (HDT, an alkanedithiolate of six methylene units) and BDT junctions with achiral and chiral gold electrodes, correlating the atomic structure with the corresponding conduction mechanisms.

In this work, we demonstrate that single-molecule junctions can indeed be built by chiral Au(5,3) nanotubes, which have similar conductance with but different transmission spectra from the ones based on Au(100) nanowires. Two kinds of thiolate-terminated molecules are chosen for the present study,

**Received:** March 13, 2013
**Revised:** June 1, 2013
**Published:** June 13, 2013

  

viz. (a) $\sigma$-saturated HDT and (b) $\pi$-conjugated BDT, to facilitate two different kinds of carbon−carbon bonds and hence the interactions. The HDT junction with the Au(5,3) nanotubes gives a broader transmission peak (thus a stronger coupling) than that with the Au(100) nanowires. In contrast, the BDT junction displays a comparable width in the transmission peak with both types of nanoelectrodes. We analyze these novel properties, in terms of the projected and local density of states, to understand the underlying physics.

## METHODS

We relaxed chiral Au(5,3) nanotube based single molecular junctions in the framework of density functional theory (DFT),[34] employing the plane-wave basis set and the generalized gradient approximation (GGA)[35] for exchange-correlation functional, with Vanderbilt ultrasoft pseudopotentials and the plane wave cutoff of 25 Ry. Each anchoring S atom was linked to the neighboring Au electrode on either side of the respective molecule. As the electrodes were moved apart in a realistic situation associated with a mechanical break junction, the respective S atom pulled the adjacent Au atoms into the periphery of chiral nanotubes leading to the formation of an atomistic Au tip. In the present study, we added a triangular cluster of three Au atoms on the edge of each prerelaxed nanotube to model the Au tip. The supercell thus included a sufficiently large part [one unit cell of the Au(5,3) nanotube or two unit cells of the Au(100) nanowire] of the electrodes bonded through the adatoms to a single molecule in between and vacuum regions with a length around 1.2 nm along the perpendicular axis. We then optimized the entire molecular moiety along with the triangular clusters while keeping the atom positions in each nanotube fixed to have energetically stable configurations for respective chiral nanojunctions. We considered the periodicity of chiral Au(5,3) nanotube through $2\pi/5$ rotation of the helical strands, by omitting a small strain along the tube, so that the number of Au atoms in the unit cell is reduced from 190 to 38, to lower the computing load.[27] On the other hand, for achiral Au(100) nanowire based single molecular junctions, an Au adatom on the edge of each nanowire was added to mimic the Au tip. The molecule along with two gold adatoms were optimized while keeping the atom positions in each prerelaxed nanowire fixed.[15] The unit cell of the Au(100) nanowire consists of nine atoms. We then stretched the electrodes, optimized it again, and continued to do so until we came up with a set of maximally stretched two-probe configurations with minimum energy and force.

The electronic transport calculations were performed using Nanodcal,[36,37] based on the nonequilibrium Green's functions approach on top of DFT, by exploiting the nonorthogonal localized double-$\zeta$ polarized basis set, within the GGA. The relaxed supercell was used as the scattering region. The transmission spectrum, $T(E)$, at a given energy $(E)$, is expressed as $T(E) = Tr[\Gamma_L(E)G^r(E)\Gamma_R(E)G^a(E)]$, where $G^{r(a)}$ denote the retarded (advanced) Green's functions of the scattering region; $\Gamma_{L(R)}(E) = \mathcal{J}[\sum^r_{L(R)}(E) - \sum^{r\dagger}_{L(R)}(E)]$ signify the line widths due to the coupling of the molecule, $\sum^r_{L(R)}(E)$, with the left (L) and right (R) electrodes, as determined from the electrode Green's functions. In the linear response regime, the conductance $(G)$ values were obtained from the Landauer formula, $G = T(E_F)G_0$, with $E_F$ being the Fermi energy and $G_0 = 2e^2/h$ being the quantum of conductance.[38] In our calculations, the electron−phonon interactions[39,40] were ignored.

## RESULTS AND DISCUSSIONS

Figure 1 shows the optimized junction geometries of HDT bonded to gold adatoms on Au(100) and Au(5,3) electrodes,

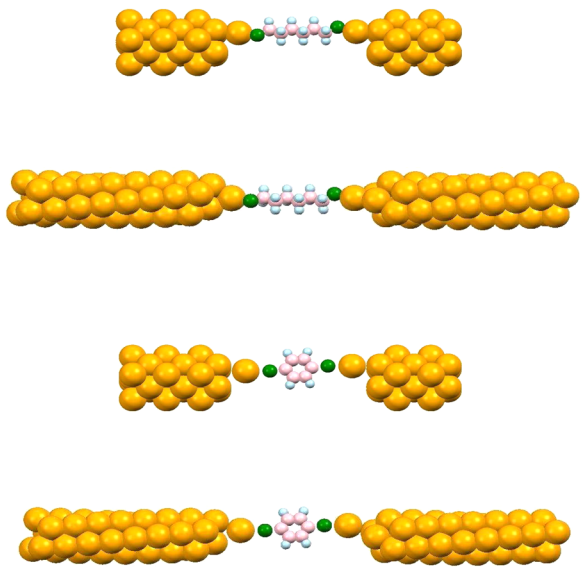

**Figure 1.** Relaxed junction geometries of hexanedithiolate bonded to gold adatoms on Au(100) and Au(5,3) electrodes and of benzenedithiolate bonded to gold adatoms on Au(100) and Au(5,3) electrodes (from top to bottom, respectively), along the $z$ axis and lying on the plane which is 45° to the $yz$ plane.

and of BDT bonded to gold adatoms on Au(100) and Au(5,3) electrodes (from top to bottom, respectively), along the $z$ axis and lying on the plane which is 45° to the $yz$ plane. With the aid of these relaxed geometries, the conductance values are calculated (see the Methods section). For the HDT molecular junctions with Au(100) and Au(5,3) electrodes, our calculated conductance values of 0.0020 and 0.0018 $G_0$ respectively come close to the experimental one of 0.0012 $G_0$.[17,18] Also, for the BDT junctions with Au(100) and Au(5,3) electrodes, our respective values of 0.015 and 0.017 $G_0$ agree well with the available measured data of 0.011[19,20] or 0.013 $G_0$.[24] The agreement with experimental values of the conductance supports the accuracy of the junction geometries and offers an opportunity to explore their conduction mechanisms.

The transmission spectrum of the Au(100)-HDT-Au(100) junction is shown in the top panel of Figure 2. As a double quantum-dot system with quantum interference,[15] two Fano resonances appear at −0.07 and −0.21 eV, dominating the junction conductance. A broader, the third, resonance locates at −0.84 eV. To investigate the character of the transmission peaks and the influence of the molecule-metal interface, we plot the projected density of states (PDOS) on the Au adatom and the S atom, along with respective orbital contributions, in the middle panel of Figure 2. It turns out that the resonances at −0.07 and −0.21 eV originate from the $p_x$ orbital of S atom and the $d_{zx}$ orbital of the Au adatom, having $\pi$ character, as these orbitals are perpendicular to the molecular bond (in the $yz$ plane). On the other hand, the resonance at −0.84 eV stems from the $p_y$ orbital of S atom and the $d_{z2}$ orbital of the Au adatom, having $\sigma$ character, as these orbitals are parallel to the molecular bond. This $\sigma$ peak is broader (full width at half-maximum) than the $\pi$ ones, indicating that the $\sigma$ channel is better coupled. While the PDOS curves hold the main features


dx.doi.org/10.1021/jp402531p | J. Phys. Chem. C 2013, 117, 13676−13680

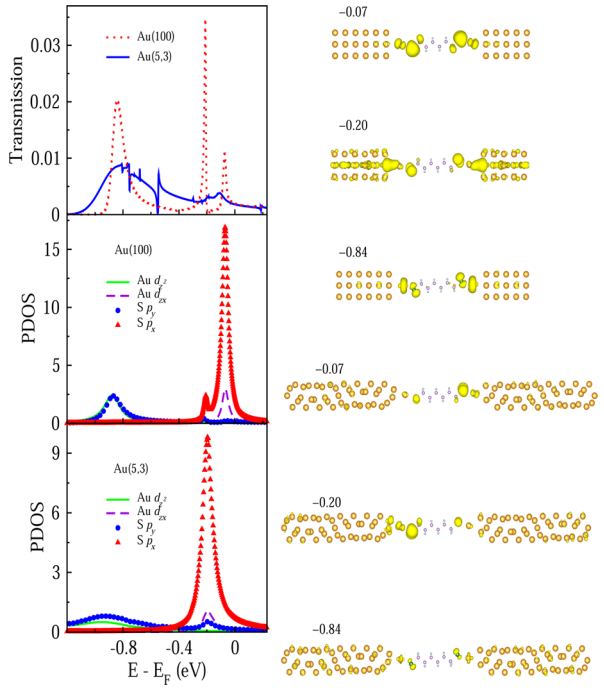


**Figure 2.** For hexanedithiolate single-molecule junctions, their transmission spectra and their projected density of states (with arbitrary units) on the gold adatom and the sulfur atom, along with respective orbital contributions. Over the junction geometries (along the *z* axis and lying on the *yz* plane) are the local density of states, with the isovalue of 0.025, for junctions with Au(100) and Au(5,3) electrodes at three featuring energies, −0.07, −0.20, and −0.84 eV. For clarifying, the size of the atom is reduced.

of the transmission spectrum and demonstrate that the molecule-metal interface is important for conduction, the PDOS-transmission variances, such as the peak heights, suggest the existence of another key factor for conduction. In the right part of Figure 2, we display the local density of states (LDOS), with the isovalue of 0.025 which gives the highest contrast, on the junctions at three featuring energies, −0.07, −0.20, and −0.84 eV. While the LDOS at the interface corresponds well with the PDOS, its distribution on the gold electrodes governs the resonance height. For example, the LDOS at −0.20 eV spans over the whole nanowires and produces the transmission maximum.

The transmission spectrum of the Au(5,3)-HDT-Au(5,3) junction is also shown in the top panel of Figure 2. Although two small resonances occur around −0.07 and −0.21 eV, the broad resonance centered at −0.83 eV dominates the junction conductance. It has $\sigma$ character (from the $p_y$ orbital of S atom and the $d_{z^2}$ orbital of the Au adatom), as the PDOS in the bottom panel of Figure 2 shows, while the small resonances have $\pi$ character. The $\sigma$ channel is still better coupled than does the $\pi$ one in this junction. The LDOS distributed on the electrodes (the right part of Figure 2) gives rise to the resonance as well. For instance, the LDOS at −0.84 eV spreads on the whole nanotubes and generates the transmission maximum. Since all resonances occur below the Fermi level, electrons tunnel through the $\sigma$-saturated HDT molecule via the $\sigma$- or $\pi$-type interface states yielding transmission peaks that are influenced by the LDOS distributed on the electrodes. To compare with the Au(100) junction, the $\sigma$ peak of the Au(5,3) junction is broader and better coupled than that in the Au(100) one. It is because the Au(5,3) nanotube holds a longer periodicity, and thus it has a incident wave with a longer wavelength (particularly for its $\sigma$ band) and owns a stronger coupling. Furthermore, while the $\sigma$ and $\pi$ resonances govern the conduction in the Au(5,3) and Au(100) junctions, respectively, they give similar conductance values. The $\sigma$ channel is better preserved in the Au(5,3) junction than in the Au(100) case, and thus the HDT molecule can act as a better momentum filter in between the Au(5,3) electrodes.

The transmission spectrum of the Au(100)-BDT-Au(100) junction is presented in the top panel of Figure 3. Two major

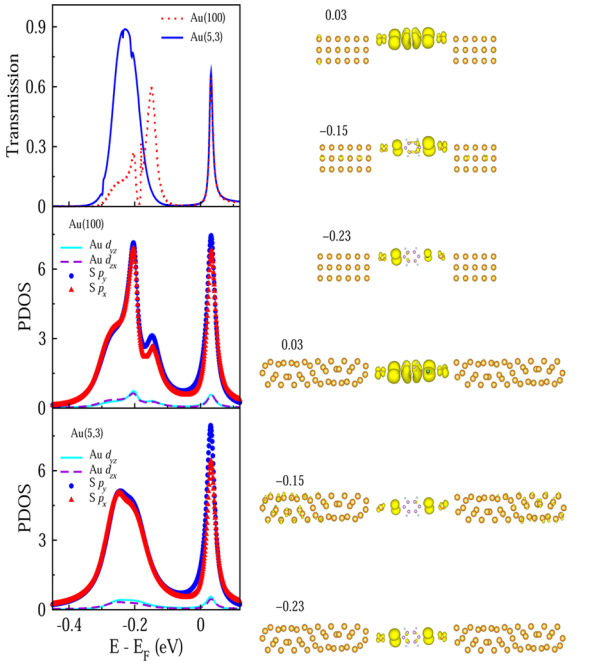


**Figure 3.** For benzenedithiolate single-molecule junctions, their transmission spectra and their projected density of states (with arbitrary units) on the gold adatom and the sulfur atom, along with respective orbital contributions. Over the junction geometries (along the *z* axis and lying on the *yz* plane) are the local density of states, with the isovalue of 0.025, for junctions with Au(100) and Au(5,3) electrodes at three featuring energies, +0.03, −0.15, and −0.23 eV. For clarifying, the size of the atom is reduced.

transmission resonances which are larger than those of the HDT junctions by an order of magnitude happen at +0.03 and −0.15 eV. These are stemmed from LUMO and HOMO, respectively. The LUMO resonance dominates the junction conductance. The PDOS curves, shown in the middle panel of Figure 3, are similar to the transmission spectrum. However, all peaks come from the $p_x$ and $p_y$ orbitals of the S atom, and the $d_{yz}$ and $d_{zx}$ orbitals of the Au adatom, where the *x*-type and *y*-type orbitals contribute almost equally. This indicates that the interface states have the $\pi$ character. In the right part of Figure 3, we show the LDOS on the junctions at three featuring energies, +0.03, −0.15, and −0.23 eV. The LDOS at 0.03 eV, which determines the junction conductance, spreads on the Au adatoms and the BDT molecule and builds a conjugated $\pi$ channel, where the d orbitals of the Au adatom are parallel with the $\pi$ orbitals of the BDT molecule. It is in sharp contrast to the LDOS at −0.07 eV of the HDT junctions (see Figure 2), where the tunneling gap in the HDT molecule dominates the junction conductance, yielding an order larger conductance in the BDT


dx.doi.org/10.1021/jp402531p | J. Phys. Chem. C 2013, 117, 13676−13680

than in the HDT junction. On the other hand, for the occupied state, electron tunneling governs the conduction properties. The d orbitals of the Au adatom are parallel with the $\sigma$ orbitals of the molecule, causing a $\sigma$ channel. The $\sigma$-type LDOS covers the benzene ring at −0.15 eV, but it is almost absent at −0.23 eV, giving a higher transmission coefficient in the former energy than in the latter energy. Importantly, in this high transmission region, the BDT molecule and the Au adatoms, rather than the electrode, dominates the conduction properties.

The transmission spectrum of the Au(5,3)-BDT-Au(5,3) junction is presented in the top panel of Figure 3 as well. Two transmission resonances occur at +0.03 and −0.23 eV. The LUMO resonance coincides with the one of the Au(100)-BDT-Au(100) junction, giving the similar conductance values. The HOMO resonance is higher than the one of the Au(100)-BDT-Au(100) junction, but their widths are similar. The PDOS curves, displayed in the bottom panel of Figure 3, present the same trend as the transmission spectrum. The contributing orbitals at the interface, as well as the LDOS (in the right part of Figure 3), are similar to those of the Au(100)-BDT-Au(100) junction. However, the $\sigma$-type LDOS extends on the benzene ring at −0.23 eV but it lacks at −0.15 eV, together with the PDOS on the interface, generating the transmission peak at the former energy. This resonance is higher than that in the Au(100) junction, as the $\sigma$ channel is better coupled in the chiral Au(5,3) junction.

## CONCLUSIONS

Chiral Au(5,3) nanotubes can potentially form stable single-molecule junctions which render similar conductance but display different transmission spectra from the ones based on achiral gold nanowires. The local density of states are essentially governed by whether $\sigma$- or $\pi$-type molecule features the major conduction channel. However, these can be further controlled by the chirality of electrodes. For the HDT junction, electrons tunnel through the $\sigma$-saturated molecule via the $\sigma$- or $\pi$-type interface states yielding transmission peaks that are influenced by the LDOS distributed on the electrode. However, in such a junction laced with Au(5,3) nanotubes, the $\sigma$-type interface states dominate the conductance, the transmission peak is broader, and the $\sigma$ channel is well preserved. On the other hand, for the BDT junction, electrons transport (tunnel) through the $\pi$ ($\sigma$) orbital of the benzene ring, mediated by the LUMO (HOMO), with the $\pi$-type interface states, generating transmission peaks that are influenced by the LDOS distributed on the molecule. While the $\sigma$ channel is better coupled in the chiral nanotube system, a higher transmission peak from the occupied state is obtained in a Au(5,3)-BDT junction.

## AUTHOR INFORMATION

### Corresponding Author

*E-mail: kauncc@gate.sinica.edu.tw.

### Present Address

[§]SRM Research Institute, SRM University, Chennai 603203, India.

### Notes

The authors declare no competing financial interest.

## ACKNOWLEDGMENTS

We thank Hong Guo and Ming-Tsung Lee for fruitful discussions. This work was partially supported by National Science Council (Contract No. 101-2112-M-001-025-MY3) and the National Center for Theoretical Sciences, Republic of China.

## REFERENCES

(1) Joachim, C.; Gimzewski, J. K.; Aviram, A. Electronics Using Hybrid-Molecular and Mono-Molecular Devices. *Nature* **2000**, *408*, 541−548.
(2) Nitzan, A.; Ratner, M. A. Electron Transport in Molecular Wire Junctions. *Science* **2003**, *300*, 1384−1389.
(3) Tao, N. J. Electron Transport in Molecular Junctions. *Nat. Nanotechnol.* **2006**, *1*, 173−181.
(4) Hu, Y. B.; Zhu, Y.; Gao, H. J.; Guo, H. Conductance of an Ensemble of Molecular Wires: A Statistical Analysis. *Phys. Rev. Lett.* **2005**, *95*, 156803.
(5) Kamenetska, M.; Koentopp, M.; Whalley, A. C.; Park, Y. S.; Steigerwald, M. L.; Nuckolls, C.; Hybertsen, M. S.; Venkataraman, L. Formation and Evolution of Single-Molecule Junctions. *Phys. Rev. Lett.* **2009**, *102*, 126803.
(6) Solomon, G. C.; Herrmann, C.; Hansen, T.; Mujica, V.; Ratner, M. A. Exploring Local Currents in Molecular Junctions. *Nat. Chem.* **2010**, *2*, 223−228.
(7) Ke, S.-H.; Yang, W. Quantum-Interference-Controlled Molecular Electronics. *Nano Lett.* **2008**, *8*, 3257−3261.
(8) Sergueev, N.; Tsetseris, L.; Varga, K.; Pantelides, S. Configuration and Conductance Evolution of Benzenedithiol Molecular Junctions under Elongation. *Phys. Rev. B* **2010**, *82*, 073106.
(9) Müller, K.-H. Effect of the Atomic Configuration of Gold Electrodes on the Electrical Conduction of Alkanedithiol Molecules. *Phys. Rev. B* **2006**, *73*, 045403.
(10) Quek, S. Y.; Choi, H. J.; Louie, S. G.; Neaton, J. B. Length Dependence of Conductance in Aromatic Single-Molecule Junctions. *Nano Lett.* **2009**, *9*, 3949−3953.
(11) Quek, S. Y.; Kamenetska, M.; Steigerwald, M. L.; Choi, H. J.; Louie, S. G.; Hybertsen, M. S.; Neaton, J. B.; Venkataraman, L. Mechanically Controlled Binary Conductance Switching of a Single-Molecule Junction. *Nat. Nanotechnol.* **2009**, *4*, 230−234.
(12) Kaun, C.-C.; Guo, H. Resistance of Alkanethiol Molecular Wires. *Nano Lett.* **2003**, *3*, 1521−1525.
(13) Kaun, C.-C; Guo, H.; Grütter, P.; Lennox, R. B. Momentum Filtering Effect in Molecular Wires. *Phys. Rev. B* **2004**, *70*, 195309.
(14) Luzhbin, D. A.; Kaun, C.-C. Origin of High- and Low-Conductance Traces in Alkanediisothiocyanate Single-Molecule Contacts. *Phys. Rev. B* **2010**, *81*, 035424.
(15) Sen, A.; Kaun, C.-C. Effect of Electrode Orientations on Charge Transport in Alkanedithiol Single-Molecule Junctions. *ACS Nano* **2010**, *4*, 6404−6408.
(16) He, J.; Sankey, O.; Lee, M.; Tao, N. J.; Li, X.; Lindsay, S. Measuring Single Molecule Conductance with Break Junctions. *Faraday Discuss* **2006**, *131*, 145−154.
(17) Xu, B.; Tao, N. J. Measurement of Single-Molecule Resistance by Repeated Formation of Molecular Junctions. *Science* **2003**, *301*, 1221−1223.
(18) Fu, M.-D.; Chen, I.-W. P.; Lu, H.-C.; Kuo, C.-T.; Tseng, W.-H.; Chen, C.-H. Conductance of Alkanediisothiocyanates: Effect of Headgroup-Electrode Contacts. *J. Phys. Chem. C* **2007**, *111*, 11450−11455.
(19) Xiao, X.; Xu, B.; Tao, N. J. Measurement of Single Molecule Conductance: Benzenedithiol and Benzenedimethanethiol. *Nano Lett.* **2004**, *4*, 267−271.
(20) Tsutsui, M.; Taniguchi, M.; Kawai, T. Atomistic Mechanics and Formation Mechanism of Metal-Molecule-Metal Junctions. *Nano Lett.* **2009**, *9*, 2433−2439.
(21) Jang, S.-Y.; Reddy, P.; Majumdar, A.; Segalman, R. A. Interpretation of Stochastic Events in Single Molecule Conductance Measurements. *Nano Lett.* **2006**, *6*, 2362−2367.
(22) Kim, Y.; Pietsch, T.; Erbe, A.; Belzig, W.; Scheer, E. Benzenedithiol: A Broad-Range Single-Channel Molecular Conductor. *Nano Lett.* **2011**, *11*, 3734−3738.

(23) Strachan, D. R.; Smith, D. E.; Fischbein, M. D.; Johnston, D. E.; Guiton, B. S.; Drndic, M.; Bonnell, D. A.; Johnson, A. T. Clean Electromigrated Nanogaps Imaged by Transmission Electron Microscopy. *Nano Lett.* **2006**, *6*, 441−444.
(24) Song, H.; Kim, Y.; Jang, Y. H.; Jeong, H.; Reed, M. A.; Lee, T. Observation of Molecular Orbital Gating. *Nature* **2009**, *462*, 1039−1043.
(25) Rodrigues, V.; Fuhrer, T.; Ugarte, D. Signature of Atomic Structure in the Quantum Conductance of Gold Nanowires. *Phys. Rev. Lett.* **2000**, *85*, 4124.
(26) Tosatti, E.; Prestipino, S.; Kostlmeier, S.; Dal Corso, A.; Di Tolla, F. D. String Tension and Stability of Magic Tip-Suspended Nanowires. *Science* **2001**, *291*, 288−290.
(27) Senger, R. T.; Dag, S.; Ciraci, S. Chiral Single-Wall Gold Nanotubes. *Phys. Rev. Lett.* **2004**, *93*, 196807.
(28) Oshima, Y.; Onga, A.; Takayanagi, K. Helical Gold Nanotube Synthesized at 150 K. *Phys. Rev. Lett.* **2003**, *91*, 205503.
(29) Kaun, C.-C.; Seideman, T. Conductance, Contacts, and Interface States in Single Alkanedithiol Molecular Junctions. *Phys. Rev. B* **2008**, *77*, 033414.
(30) Paulsson, M.; Krag, C.; Frederiksen, T.; Brandbyge, M. Conductance of Alkanedithiol Single-Molecule Junctions: A Molecular Dynamics Study. *Nano Lett.* **2009**, *9*, 117−121.
(31) Toher, C.; Sanvito, S. Effects of Self-Interaction Corrections on the Transport Properties of Phenyl-Based Molecular Junctions. *Phys. Rev. B* **2008**, *77*, 155402.
(32) Strange, M.; Rostgaard, C.; Häkkinen, H.; Thygesen, K. S. Self-Consistent GW Calculations of Electronic Transport in Thiol- and Amine-Linked Molecular Junctions. *Phys. Rev. B* **2011**, *83*, 115108.
(33) Pontes, R. B.; Rocha, A. R.; Sanvito, S.; Fazzio, A.; da Silva, A. J. R. Ab Initio Calculations of Structural Evolution and Conductance of Benzene-1,4-dithiol on Gold Leads. *ACS Nano* **2011**, *5*, 795−804.
(34) Giannozzi, P.; Baroni, S.; Bonini, N.; Calandra, M.; Car, R.; Cavazzoni, C.; Ceresoli, D.; Chiarotti, G. L.; Cococcioni, M.; Dabo, I.; et al. QUANTUM ESPRESSO: A Modular and Open-Source Software Project for Quantum Simulations of Materials. *J. Phys.: Condens. Matter* **2009**, *21*, 395502.
(35) Perdew, J. P.; Burke, K.; Ernzerhof, M. Generalized Gradient Approximation Made Simple. *Phys. Rev. Lett.* **1996**, *77*, 3865.
(36) Taylor, J.; Guo, H.; Wang, J. Ab initio Modeling of Quantum Transport Properties of Molecular Electronic Devices. *Phys. Rev. B* **2001**, *63*, 245407.
(37) Waldron, D.; Haney, P.; Larade, B.; MacDonald, A.; Guo, H. Nonlinear Spin Current and Magnetoresistance of Molecular Tunnel Junctions. *Phys. Rev. Lett.* **2006**, *96*, 166804.
(38) Landauer, R. Conductance Determined by Transmission: Probes and Quantised Constriction Resistance. *J. Phys.: Condens. Matter* **1989**, *1*, 8099.
(39) Pecchia, A.; Di Carlo, A. Atomistic Theory of Transport in Organic and Inorganic Nanostructures. *Rep. Prog. Phys.* **2004**, *67*, 1497−1561.
(40) Pecchia, A.; Di Carlo, A.; Gagliardi, A.; Niehaus, T. A.; Frauenheim, T. Atomistic Simulation of the Electronic Transport Organic Nanostructures: Electron-Phonon and Electron-Electron. *J. Comput. Electron.* **2005**, *4*, 79−82.